

Erosive Burning of Solid Rocket Propellants—A Revisit

Ellis M. Landsbaum*

The Aerospace Corporation, Los Angeles, California 90009-2957

A solid-propellant rocket motor test that exhibited unexpected erosive burning led to an extensive literature review of the subject. A qualitative theory that explains why higher burning-rate propellants are less prone to erosive burning, why propellants with similar burn rates have similar erosive behavior, and why erosive burning decreases as motor size increases evolved. The decrease in erosive burning with increasing motor size is caused by a decrease in the gas velocity that causes turbulence at the flame zone. This is predicted based on equations for the developing laminar boundary-layer velocity profile on a flat plate in compressible flow. The erosive burning data in the literature correlate well with the specific mass velocity, and useful equations for the ballisticians are provided.

Nomenclature

C_p	=	heat capacity, cal/g K
D	=	diameter, cm
G	=	specific mass flow, kg/m ² s
G^*	=	value of G that results in $M = 1$ in a constant-area channel, kg/m ² s
H	=	Rectangular channel half-height, cm
K, k	=	constants
k_g	=	gas conductivity, cal/cm-s-K
M	=	Mach number
n	=	pressure exponent in burn-rate equation
P	=	pressure, MPa
Q	=	heat-release requirement, cal/cm ² s, cal/g
R	=	radius, cm
Re	=	Reynolds number
R^2	=	correlation coefficient
r	=	burn rate, cm/s
T	=	temperature, K
U	=	average channel velocity, m/s
u_λ	=	axial gas velocity at edge of flame zone, m/s
u^*	=	friction velocity, m/s (see Ref. 17)
x	=	length of boundary layer, cm
y	=	distance away from burning propellant, cm
z	=	input constant
α	=	constant in Lenoir–Robillard equation
β	=	blowing parameter in Lenoir–Robillard equation
δ	=	boundary-layer thickness where $u = 0.99U$
λ	=	flame zone thickness, cm
ν	=	kinematic viscosity, m ² /s
ρ	=	density, kg/m ³
τ_w	=	shear stress at wall, kgf/m ²

Subscripts

c	=	core
e	=	erosive burning rate
g	=	gas
h	=	hydraulic
o	=	nonerosive conditions
p	=	pyrolysis

s	=	solid
T	=	total
t	=	turbulent
th	=	threshold, $r_e = 0$ or indicates where r_e starts to increase
λ	=	at edge of flame zone

Introduction

AN unexpected occurrence of erosive burning in a development test of a solid-propellant rocket motor resulted in an extensive review of the literature. Erosive burning is the increase in the propellant burning rate in a motor as a result of the high velocity of combustion gases flowing over the surface. The Saderholm¹ data were correlated and predicted the erosive behavior very well. A review of the literature showed there was little other information of practical use for the ballisticians and little data that could be correlated like the Saderholm data. During this extensive review, a qualitative theory that shows why increasing propellant burn rate reduces erosive burning and why erosive burning decreases with increasing motor size was developed. A procedure for correlating erosive burning data that yields useful equations for the ballisticians was also developed.

Unexpected Erosive Burning

An unexpected appearance of erosive burning occurred recently. The predicted and actual pressure traces are shown in Fig. 1. The first 10 s are shown. The initial pressure was 20% above the contractors pretest prediction using SPPTM (Ref. 2). The Saderholm¹ results were correlated as shown in Fig. 2 for use in an Aerospace post-test CFD analysis. The equations for Saderholm's low burn rate propellant are given in Table 1. The line for 8.27 MPa was used in the computational-fluid-dynamics (CFD) analysis. There appears to be a threshold (minimum value for erosive burning) Mach number. The specific mass flow G_c for that condition is also given, assuming the propellant is 68% ammonium perchlorate (AP), 18% aluminum (Al), and 14% hydroxyl-terminated polybutadiene (HTPB).

The analysis was extremely successful at reproducing the test results. Details of the analysis are presented by Wang et al.³ The Aerospace CFD calculated peak pressure was within 1% of the experimental measurement. Although fortuitous, it can be explained. The width of the aft slots was similar to the diameter of the tube in Saderholm's experiment; therefore, the gas velocity distribution would be similar. The propellant burn rates were similar, and there appears to be general agreement that propellants of similar burn rates have similar erosive burning.⁴

The contractor's pretest misprediction (Fig. 1) occurred because if the SPPTM (Ref. 2) input file does not contain a value for β the erosive burning module is bypassed even though β does not appear in the Saderholm equations. There is another problem with the Saderholm equation. The equation is given as

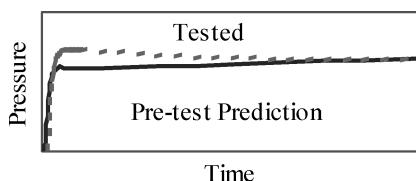
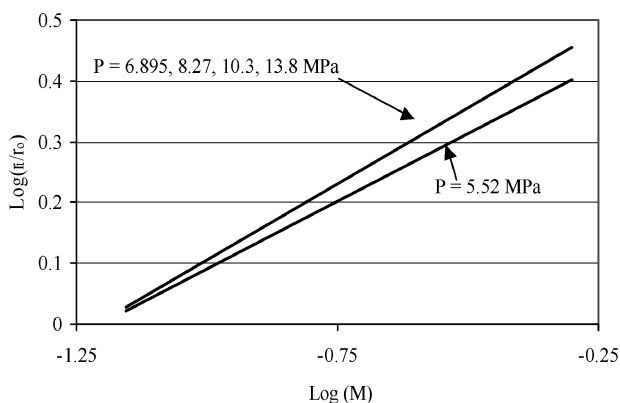
$$r_T/r_o = 1.037(M/M_{th})^z(1.2/D_h)^{0.2} \quad (1)$$

Presented as Paper 2003-4805 at the AIAA/ASME/SAE/ASEE 39th Joint Propulsion Conference and Exhibit, Huntsville, AL, 20–23 July 2003; received 15 September 2003; revision received 7 October 2004; accepted for publication 3 September 2004. Copyright © 2004 by The Aerospace Corporation. Published by the American Institute of Aeronautics and Astronautics, Inc., with permission. Copies of this paper may be made for personal or internal use, on condition that the copier pay the \$10.00 per-copy fee to the Copyright Clearance Center, Inc., 222 Rosewood Drive, Danvers, MA 01923; include the code 0748-4658/05 \$10.00 in correspondence with the CCC.

*Senior Engineering Specialist, P.O. Box 92957—M4/969. Associate Fellow AIAA.

Table 1 Saderholm¹ data fit equations $r_T/r_o = K1(M)^{K2}$

P , MPa	$K1$	$K2$	M_{th}	G_c , kg/m ² s
5.516	3.43	0.443	0.06236	365
6.895	3.88	0.481	0.05951	435
8.274	4.02	0.499	0.06147	538
10.343	4.06	0.504	0.06199	677
13.79	4.1	0.511	0.06346	924

**Fig. 1** Motor test showing unexpected erosive burning.**Fig. 2** Correlation of Saderholm's¹ data.

where D_h is in inches. D_h can become sufficiently large to reduce the burn rate; this occurred with the motor of Fig. 1, and the constant 1.037 cannot be changed. Care should be used for predictions with SPP (Ref. 2) with noncircular port designs if erosive burning is expected because it is a one-dimensional program and the Mach number varies with radial location in these designs. Therefore, a CFD analysis is preferred for the ballistic analysis with erosive burning of any propellant grain with a noncircular port. A casual perusal of the erosive burning literature showed there was nothing very useful to the ballisticians. An extensive review of all of the literature since Green⁵ led to the results presented here.

Theory

The theory to be presented is qualitative and based on the Lenoir and Robillard⁶ (L&R) evaluation that erosive burning is caused by additional heat flux to the propellant. Essentially all subsequent theoretical studies have been about the source of the additional heat and how to calculate erosive burning. This study does not resolve that question but does result in useful information for the ballisticians. One can write

$$Q_t = k_{gt} \left(\frac{dT}{dy} \right)_t - k_{go} \left(\frac{dT}{dy} \right)_o \quad (2)$$

where Q_t is the additional heat generated by turbulence or other factors. Turbulence increases dT/dy above the normal value. Razdan and Kuo⁷ (R&K) explain that the turbulence increases the mixing of fuel and oxidizer streams bringing them closer to the surface and also increases the transport of heat to the propellant. The effect of turbulence is to increase heat flow, which increases the burning rate. Equation (2) leads to

$$r_e = Q_t / \rho_s Q_p \quad (3)$$

Table 2 Heats of pyrolysis^a

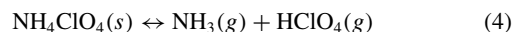
Ingredient	Q_p , cal/g	Ref. no.
AP	567	8
Polysulfide	140	9
Polyurethane	151	9
Polyester	151	— ^b
Polystyrene	346	10
CTPB	2084	9
PBAA	2024	9
PBAN	2024	— ^c
HTPB	850	11

^aThe heat required to raise the ingredient from 25 to 300°C is included. $C_p = 0.395$ cal/g·K was used for all polymers.

^bAssumed same as polyurethane.

^cAssumed same as PBAA.

Q_p of major propellant ingredients are given in Table 2. (Aluminum poses a problem, as will be discussed.) The AP value is based on 58 kcal/gmol for the following reaction⁸:



The HTPB value includes the appropriate amount of dimethyl diisocyanate and is based on 43 kcal/gmol to break a single bond in polybutadiene¹⁰ and assumes every fourth bond is broken.

Equation (3) explains simply why faster burning propellants appear less prone (the percentage that is erosive burning is less) to erosive burning—a concept from early ballisticians. Consider two similar propellants, A and B, where B burns twice as fast as A. Under a given set of flow conditions, erosive burning of A is 20% of the base value. Under those same conditions the erosive burning for propellant B will be about the same, but now only 10% of the base value. Further, it will be more difficult to increase Q_t for the faster burning propellant because the reaction rate must already be high to result in a higher burn rate, and in the analysis to follow the turbulence will be less for the faster burning propellant because the gas velocity will be less at the edge of the flame zone. Therefore, the erosive burning for propellant B will be less than 10% of its base value. This is also a partial explanation of why propellants with similar burn rates have similar erosive behavior.⁴ Q_p and ρ_s are similar for most propellants. At all flow conditions Q_t will be similar for propellants of similar burn rates. The result is that the erosive behavior is also similar. Although there is a wide range of Q_p for the different ingredients, AP dominates the calculation for a propellant, and the value for different propellants is not that dissimilar.

The correlation procedure that follows started by assuming that the turbulent intensity and the additional heat can be related by an equation¹² similar to the Lenoir–Robillard equation,⁶

$$Q_t = K G^{0.8} \exp(-\beta r_t \rho_s / G) \quad (5)$$

Razdan and Kuo,⁷ King,¹³ and Beddini¹⁴ all note that in calculating Q_t caused by turbulent intensity one must use the local flow conditions. King¹³ and Beddini¹⁴ have presented the effect of larger bore diameters on erosive burning, but the procedures are difficult for a ballisticians to use. The Beddini analysis was evaluated for use in SPP (Ref. 2) and without an explanation resulted in a suggested motor diameter effect, which will be presented later.

This analysis uses the gas velocity at the edge of the flame zone. The flame zone thickness λ_o is calculated following an early suggestion¹⁵:

$$\lambda_o = k_g (T_f - T_s) / r_o \rho_s Q_p \quad (6)$$

Because erosive burning is being analyzed, one would expect r_T to be used in Eq. (6). However, r_T frequently gave poorer correlations as measured by the correlation coefficient R^2 than r_o in the preliminary work of this paper. The range of flame zone thicknesses using r_o is about 10 to 30 μ , much less than the frequently suggested value of $\sim 100 \mu$. λ_o should be considered as a representative thickness as opposed to an actual value. T_f and k_g are the values for the combustion

products obtained from TEPTM (Ref. 16). The thermal conductivity is lower in the flame zone than for the combustion products so that this procedure underestimates the flame zone thickness. The poorer correlations obtained using r_T are probably the result of calculating a thinner flame zone. The surface temperature T_s is 300°C for all propellants because the decomposition temperature for ammonium perchlorate does not vary much from that value with burn rate.¹⁷ Equation (6) can be reformulated to account for the heat transfer from radiation, but the effect on λ_o is small.

The gas velocity for the laboratory experiments is determined from turbulent theory¹⁸:

$$\delta/x = 0.16 / (Re_x)^{1/7} \quad (7)$$

$$u_\lambda = 0.99U(\lambda_o/\delta)^{1/7} \quad (8)$$

When motor tests were analyzed, the gas velocity was determined from Culick's¹⁹ analysis as rearranged by Dunlap et al.²⁰ and with U_c replacing U_{\max} .

$$u_\lambda = (\pi/2)U_c \cos[(\pi/2)(1 - \lambda_o/R)^2] \quad (9)$$

This appears to explain the effect of motor size on erosive burning because as R increases u_λ decreases. A similar expression was derived by Yamada et al.¹² for rectangular channels,

$$u_\lambda = (\pi/2)U_c \cos[(\pi/2)(1 - \lambda_o/H)] \quad (10)$$

This indicates the velocity will fall off more rapidly in ports designed with slots or stars and the erosive burning will be less in these designs than in circular ports such as used in all of the larger space launch motors.

Correlation of Erosive Burning Data

The Razdan and Kuo⁴ review listed 19 papers with experimental data. A similar number have been published since their review. Most of the papers were not useful for analysis purposes because there is insufficient information about the propellant, the test conditions, or erosive burning measurements. Pressure time traces from motors that exhibited erosive burning are difficult to analyze even if all of the information is available. The data analyzed were obtained by digitizing the graphical presentations. There were very few tables of data.

The analyses started with attempting to correlate King's²¹ data with the L&R⁶ equation with $G_\lambda = \rho_g u_\lambda$. Three different equations were tried,

$$\ln(r_e/G_\lambda^{0.8}) = \ln(K) - \beta r_T \rho_s / G_\lambda \quad (11)$$

$$r_e = K G_\lambda^{0.8} \exp(-\beta r_T \rho_s / G_\lambda) \quad (12)$$

where β is varied to obtain the maximum R^2 , and one can also fit both variables at the same time,

$$\ln(r_e) = K_1 + K_2 \ln(G_\lambda) - \beta r_T \rho_s / G_\lambda \quad (13)$$

Usually β was negative. A positive β could be obtained by eliminating the higher velocity data, but this is not desirable. There were some propellants that gave positive β , but the standard errors were greater than 100% of the value. All subsequent efforts correlated r_e with either G_λ or G_c and used \log_{10} .

King's review²¹ presented information on 11 different propellants. All had HTPB binders. Three formulations were AP/73% at three different burn rates as a result of using AP particle sizes of 5, 20, and 200 μ , formulations 4685, 4525, and 5051, respectively. The correlations are shown in Fig. 3. Formulation 5051 appears to coincide with formulation 4525. However, because 5051 is a slower-burning propellant, the erosive burning percent is much higher. Similar results were found for the other formulations. The results are in Table 3 except for the very fast-burning formulation 5555, which had negligible erosive burning.

Table 3 Correlation of King's²¹ data

Designation	Formulation	Other	Log(r_e) = K_1 + $K_2 \log(G_\lambda)$		R^2
			K_1	K_2	Coefficient correlation
5565	82	—	-3.606	1.1452	0.937
7993	82	—	-2.698	0.8585	0.782
7996	82	—	-3.189	1.003	0.770
8019	82	—	-3.888	1.2178	0.845
5542	77	—	-3.736	1.1236	0.911
4869	72	2%	-2.259	0.7546	0.946
		Fe ₂ O ₃			
6626	74	5% Al	-2.831	0.8488	0.933

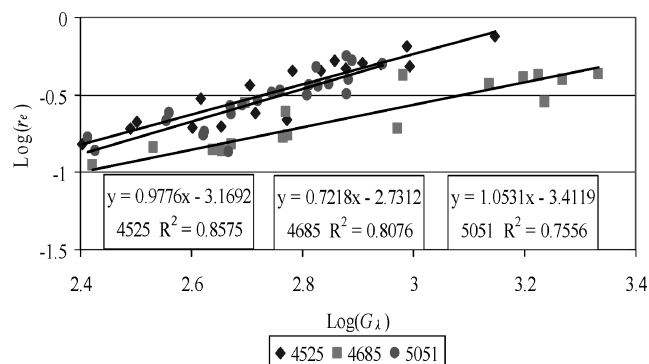


Fig. 3 Correlation of King's²¹ 73% AP/27% HTPB formulations.

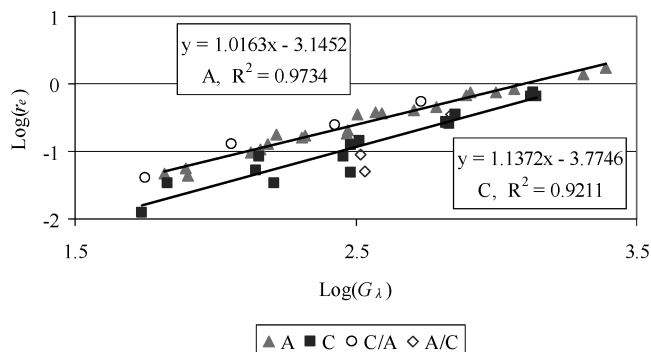


Fig. 4 Correlation of Marklund and Lake's²² data.

The results of Marklund and Lake²² (M&L) have often been cited as refuting the Lenoir-Robillard⁶ analysis because the measured erosive burning was the same even though the core gas temperature was different. However, those discussions never considered the fact that a higher temperature gas will have a lower density and therefore a lower G . The analysis of the M&L data is presented in Fig. 4. Propellant A is a 65% AP polyester propellant. M&L gave $T_f = 1690$ K. TEPTM (Ref. 16) gave 1400 K assuming $\frac{1}{3}$ of the binder was polystyrene. The gas density was corrected to the higher temperature. Propellant C is a 75% AP polysulfide-epoxy propellant. M&L gave $T_f = 2550$ K, and TEP (Ref. 16) gave 2540 K. There were four tests, labeled C/A, in which the core gas was propellant C and the test specimen was propellant A. Comparing those results to the correlation of propellant A, the average increase in r_e is 22%. This is less than the 77% increase of $\Delta T = (T_f - T_s)$. There were three tests, labeled A/C, in which the core gas was propellant A and the test specimen was propellant C. Comparing these results to the correlation of propellant C, the average decrease in r_e is 34%, which is comparable to the 44% reduction in ΔT . Therefore, when the effect of specific mass flow is considered it appears that some of the erosive burning might be caused by heat flow from the core gas as proposed by Lenoir and Robillard.⁶ Laboratory tests with N_2 as the core gas might help in determining how much of erosive

burning is caused by heat flux from the core gas and how much is caused by the increase in turbulence. This is mainly of interest to the theoreticians because the correlations with G_λ or G_c include the effect of heat transfer from the core gas.

Strand studied erosive burning with a variety of collaborators. Experiments with a Jet Propulsion Laboratory (JPL) version of the reusable solid rocket motor (RSRM) propellants were done with a Bates motor²³ and with a smaller motor called the 5×10 (Refs. 24 and 25). The Bates motor data were tabulated. The head-end pressure and r_o were given at 1-s intervals, and for the midpoint of each segment the U and r_T were given as well. This allowed an easy determination of r_e , ρ_g , and u_λ [from Eq. (9)]. The correlation is presented in Fig. 5. There appears to be a threshold effect. The analysis of the 5×10 four segment test was more difficult. There were graphs of pressure vs time at four locations and r_T/r_o at the midpoint of each segment. This required determination of burn areas and port areas vs time and resulted in the correlation in Fig. 6. The two tests are in reasonable agreement, which can be seen if the data are plotted on the same graph. The RSRM aft-end static pressure at ignition is about 5.17 MPa, $M \sim 0.25$, and $G_c \approx 1460 \text{ kg/m}^2\text{-s}$. The effect of motor diameter can be calculated using Eq. (9) (assuming segmentation has no effect) and is shown in Fig. 7. The RSRM with a port diameter of about 200 cm would have an r_e between 0.005 and 0.056 cm/s. There was a NASA paper about erosive burning in the first static test motor.²⁶ However, there was insufficient information to allow a comparison to the value presented here.

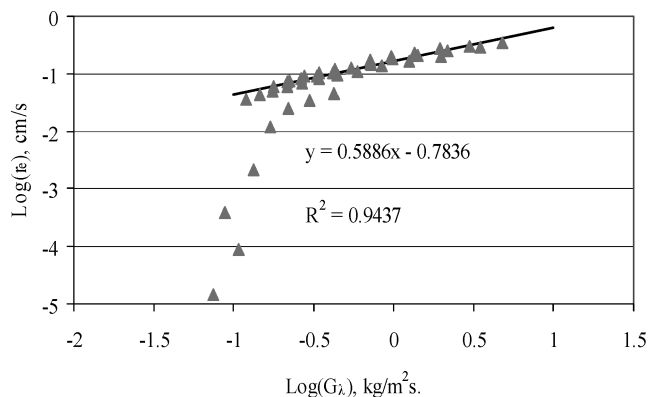


Fig. 5 Correlation of Strand et al.'s²³ Bates data.

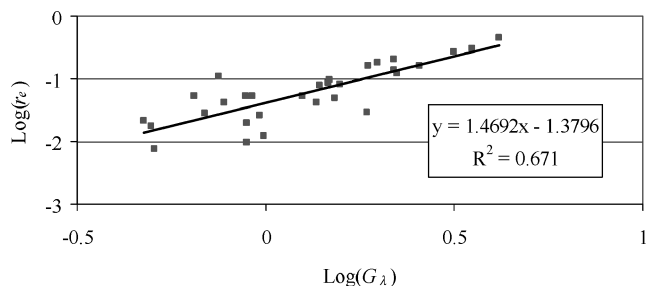


Fig. 6 Correlation of Strand and Cohen's²⁴ 5×10 data.

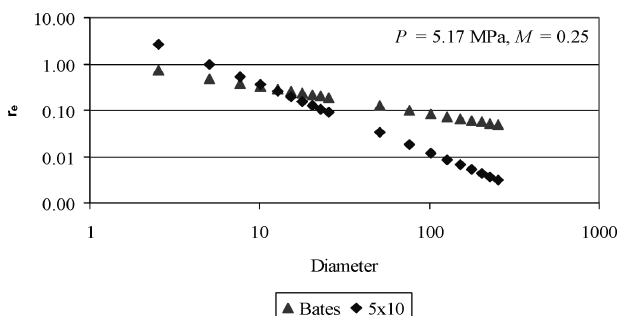


Fig. 7 Prediction of erosive burning as a function of port diameter.

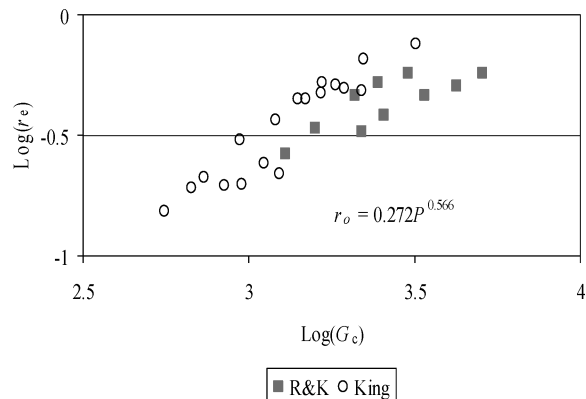


Fig. 8 Comparison of Razdan and Kuo's²⁸ and King's²¹ results for formulation 4525.

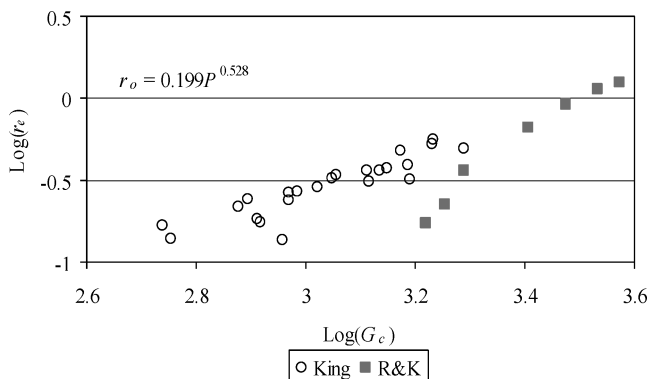


Fig. 9 Comparison of Razdan and Kuo's²⁸ and King's²¹ results for formulation 5051.

One of the problems in analyzing the RSRM propellant was the effect of aluminum on the calculation of Q_p . Although the surface temperature used in this paper is far below the melting point of aluminum, it is known that aluminum will melt and coalesce on the surface.²⁷ The heat of melting should be incorporated into Q_p , but it was not clear how this fits into Eqs. (3) and (6). Therefore, the melting heat was ignored, and only the heat necessary to raise the aluminum to the surface temperature, 59 cal/g, was used to calculate Q_p .

There are data on a number of propellants where insufficient information is given to allow the calculation of G_λ , but one can show a good correlation with G_c . A reasonable assumption is that if one can estimate u_λ a good correlation would be obtained with G_λ . Razdan and Kuo²⁸ tested two of the same propellants that King did. The results are given in Figs. 8 and 9. G_c was used because it was difficult to calculate G_λ for Razdan and Kuo's tests. The results are generally comparable. The nonerosive burn rate was determined from King's data and not the one quoted by R&K. This illustrates that the different experimental techniques give similar results.

One of the earliest erosive burning tests was conducted by Green.⁵ The results were presented as r_T vs the average G_c . This was easily converted to $\log(r_e)$ vs $\log(G_c)$, as shown in Fig. 10. The burn rate at the head-end of the motor was used as r_o . The slope of the line should be steeper because the actual r_o down the grain toward the nozzle should decrease because the static pressure decreases. The bore was tapered toward the nozzle to try and obtain a relatively constant average port area with length during the burn. A polyurethane propellant with 74% AP matched the given T_f . The propellant combustion data from TEP (Ref. 16) was used to calculate G_λ , but the results did not show an improvement over Fig. 9. The plot shows evidence of a threshold at $G_c \approx 176 \text{ kg/m}^2\text{-s}$ and $r_e \approx 0.020 \text{ cm/s}$. The threshold might be caused by the melt layer on the surface of polyurethane propellants. Thresholds will be discussed later. Green⁵

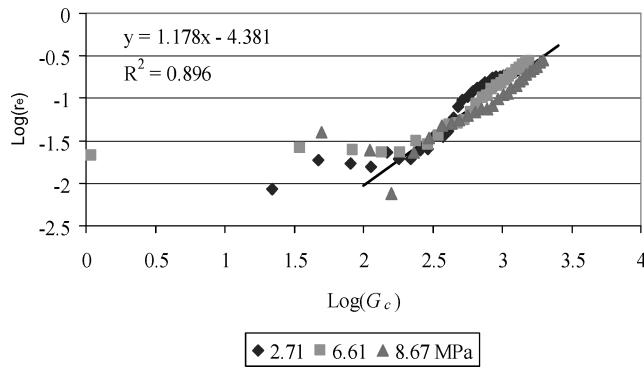


Fig. 10 Correlation of Green's⁵ data.

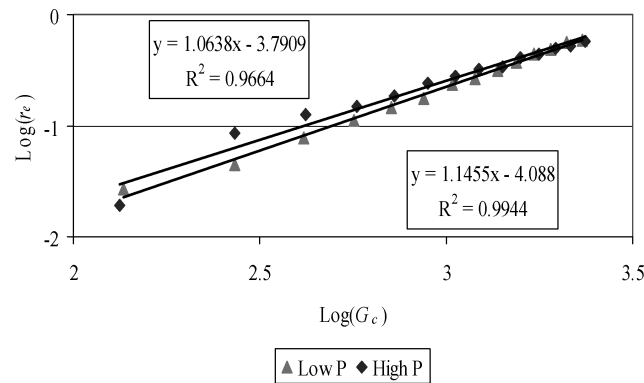


Fig. 11 Correlation of JPL 126 (Ref. 29).

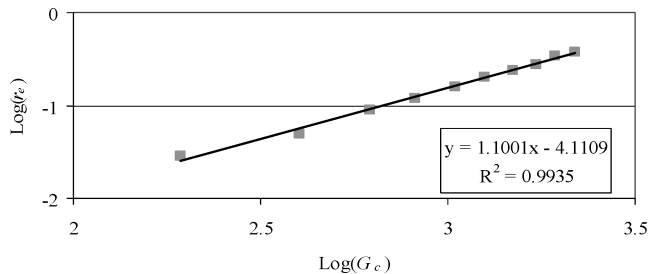


Fig. 12 Correlation of JPL 131 (Ref. 29).

presents the following equation (nomenclature of this paper):

$$r_T/r_o = 1 + kG_c/G_c^* \quad (14)$$

This is easily rearranged to

$$r_e = kr_o G_c/G_c^* \quad (15)$$

and Green's data shows that kr_o is relatively constant so that r_e is primarily a function of G_c .

Lenoir and Robillard did not provide any useful experimental data in their public report⁶ but did in a JPL report.²⁹ They tested 30 interrupted burning motors and gave seven results similar to the one in the paper. Two were star grains with insufficient geometric information. The others were tubular grains, and the data given were analyzed using Green's⁵ procedure. The results are shown in Figs. 11–13. The JPL polyurethane, JPL 527, does not show a threshold effect but does not go to as low a mass flow as Green's tests.

The French^{30–32} adopted Green's method of analysis to some extent and plotted the erosive constant r_T/r_o against G_c . The average exponent from the correlations presented here is near one so that it is not surprising a linear plot is satisfactory. Reviewing the plots in their papers, the XLDB and NEPE propellants appear to correlate with G_c like the composite propellants.

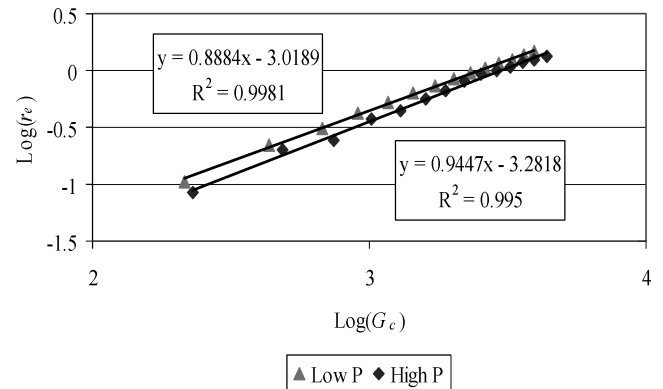


Fig. 13 Correlation of JPL 527 (Ref. 29).

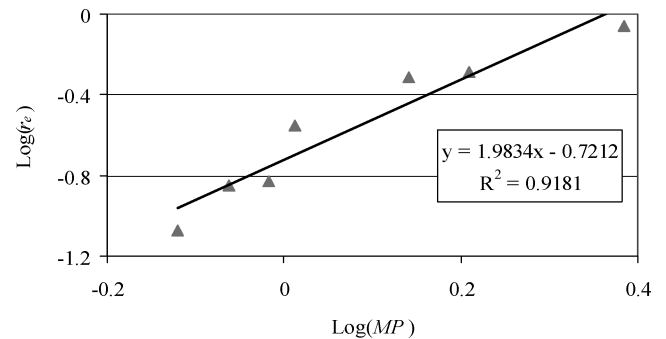


Fig. 14 Correlation of propellant NOS-1 (Ref. 34).

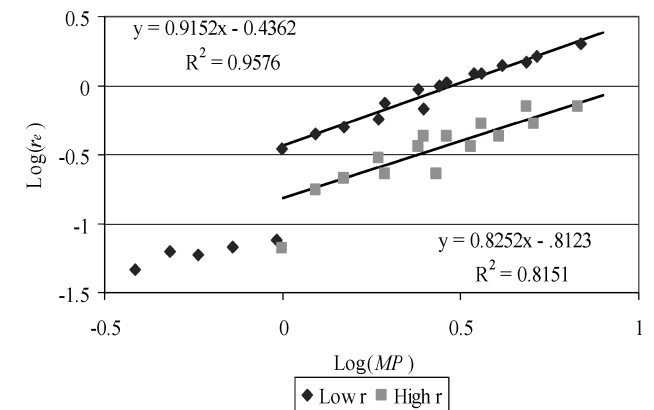


Fig. 15 Correlation of Saderholm's¹ data.

G_c is proportional to Mach number times chamber pressure, and plots of $\log(r_e)$ vs $\log(MP)$ are useful when the propellant information is not available because the slope is obtained. Kamath et al.³³ measured erosive burning of a double-base propellant (Fig. 14). The Saderholm¹ data are also correlated with MP (Fig. 15) and better illustrates an apparent threshold effect than the equations of Table 1.

Boundary-Layer Velocities

While correlating Strand's Bates data, it was noticed that the velocities from Eq. (9) were much lower than those from Eq. (8), yet the erosive behavior of the propellants was similar. A comparison of Strand's Bates data and King's 4525 data using the core gas flow shows they give similar erosive burning at these conditions, as shown in Fig. 16. Because King used a strip of propellant, it was thought this might behave more like a motor. However, M&L propellant A gives a similar comparison, as shown in Fig. 16. All of the laboratory experimental results correlated well with G_c . However, this is not useful for investigating scaling. Because the erosion rates are similar under similar core environments, the local velocities, actually G_λ ,

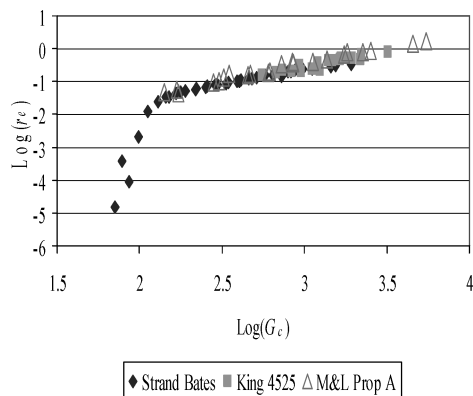


Fig. 16 Comparison of Strand's Bates, King's 4525, and M&L's propellant A data at core flow conditions.

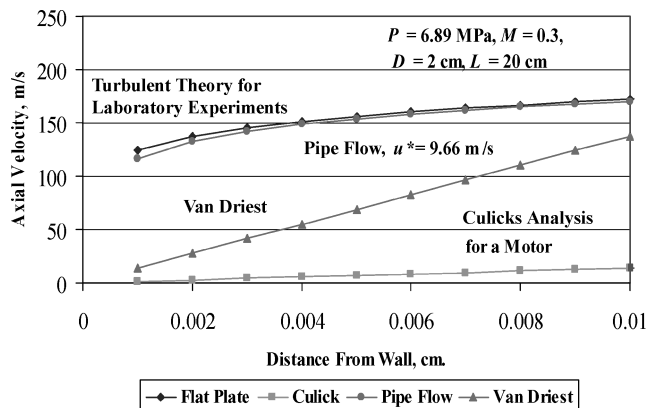


Fig. 17 Velocity profiles.

must also be similar. Further, because there is general agreement that erosive burning is caused by increased turbulence near the flame zone, and large motors have less erosive burning, the turbulence at the flame zone must be less in large motors. Thus, the criteria for the boundary-layer velocity profile are that it must give similar results for the laboratory experiments and comparable motors and the velocity must decrease significantly between small and large motors. This led to an examination of the various velocity profile "laws" that might apply.

Gas velocity vs distance from the wall is shown for different laws in Fig. 17. The conditions shown can apply to either the laboratory experiments or to a motor. The upper curve is from turbulent boundary-layer growth [Eq. (8)]. The bottom curve is from Culick's analysis [Eq. (9)]. Equation (9) is probably only accurate outside the turbulent zone.

The major problem with the use of Eq. (9) is that it gives very low velocities in the combustion zone that are much lower than the ones calculated for the laboratory experiments using Eq. (8). Each of the velocity profile equations can be evaluated for its application to scaling. Using King's 4525 as an example, one calculates $\lambda_o = 7.4 \mu$ from Eq. (6) and $u_\lambda = 118$ m/s from Eq. (8). If the dimensions are increased by a factor of 100, approximately shuttle size, λ_o is the same, but u_λ only decreases to 67 m/s, and the erosion rate would still be substantial. Assuming fully developed turbulent flow as in a pipe, the effect of motor diameter on the velocity distribution was calculated. The distribution is the same with blowing as without.³⁴ There is one problem with this concept. The equations have a term τ_w , the shear stress at the wall. Because this should be near zero for blowing, it is not clear how the same equation can apply to blowing and nonblowing boundary layers. Neglecting this problem, the velocity profile calculated for the laboratory tests with a pipe flow analysis of fully developed turbulent flow, $u^* = 9.66$ m/s, agrees with that from a developing turbulent boundary layer. Increasing the motor diameter from 2 to 200 cm will decrease u_λ by about 50%.

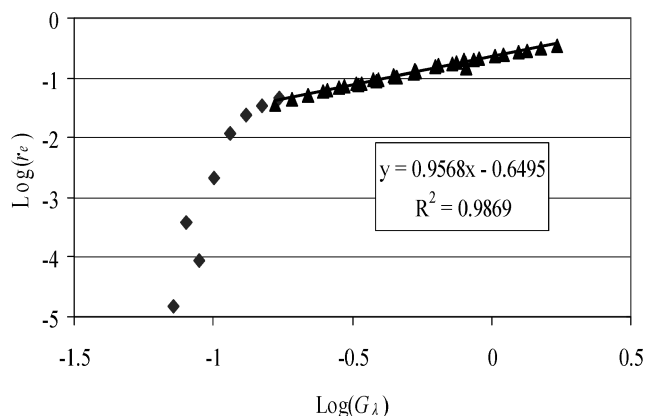


Fig. 18 Correlation of Strand's Bates data using Van Driest's velocity.

This will only decrease r_e by about 50%. A decrease of about 90% is needed to agree with large motor observations.³⁵ One can also apply the velocity defect³⁶ law and obtain similar results.

It appears that the difficulty in explaining the low erosive burning rates in large motors is caused by concentrating on the turbulent layer although the combustion zone lies entirely within the laminar sublayer. The analysis of Van Driest^{37,38} resolves the problem. Velocity profiles were calculated for the developing laminar layer along a flat plate in compressible flow. The following equation at low Mach numbers is appropriate for the linear portion of the curve, which applies to the current problem:

$$u_\lambda = 0.3U_{\lambda_o}\sqrt{(U/v/x)} \quad (16)$$

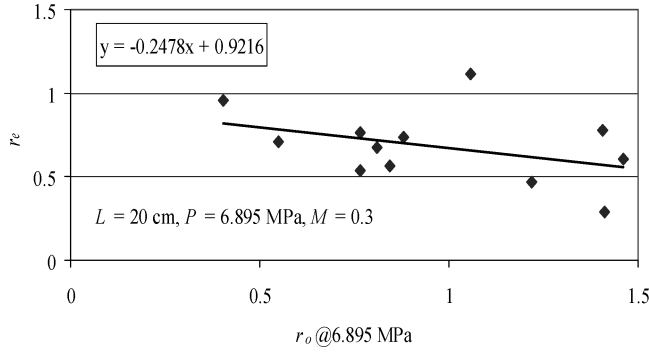
This is identical to the Blasius analysis for incompressible flow.³⁷ If one applies Eq. (16) to Strand's Bates data and assumes the boundary layer starts at the front of the fourth segment, $u_\lambda = 43.6$ m/s ($\lambda_o = 24 \mu$). This analysis applied to the shuttle aft segment gives $u_\lambda = 8.4$ m/s. Comparable numbers from Eq. (9) are 1.2 and 0.07 m/s. The large reduction in velocity explains the lower erosive burning of the shuttle and other large motors. Using Eq. (16) instead of Eq. (8) in correlating Strand's data improved the transition from threshold to turbulent values (Fig. 18). The correlation coefficient increased slightly for the Bates data and decreased slightly for the 5×10 data. It was assumed the boundary layer started at the front of a segment for both cases. Starting the boundary layer at the front of the motor resulted in poorer correlations for both sets of data. Some of the laboratory data did not correlate well using the Van Driest velocity profile. This might be the result of the curved entrance section in the apparatus. It is clear that a better understanding of the boundary-layer velocity profile is necessary to better understand erosive burning and a scaling method. The important result of the correlations presented is to show that r_e correlates with G_λ . Correlations of r_e with G_c were quite good and indicate that a correlation with G_λ is highly likely but are not useful for scaling or grain design.

Threshold Effect

Strand presented several papers on a threshold Reynolds number, the latest being Ref. 25. Beddini³⁵ also considered the subject. There are only three examples of a threshold effect in the data discussed here: the results of Green (Fig. 10); Strand (Fig. 5); and Saderholm (Table 1 and Fig. 15). The Green and Strand results are comparable with G_{th} (core) ≈ 176 and 141 kg/m²s, respectively. The respective r_e are 0.02 and 0.04 cm/s. The Saderholm G 's are all much higher. The only other specific mass flows comparable to the Green and Strand data are a few of Marklund and Lake's tests. These do not show any threshold effect. There does not appear to be a gas density influence in the data suggesting a threshold effect; note Green's data (Fig. 10), and the relatively constant M_{th} of Saderholm (Table 1). The likely cause is that the boundary-layer axial velocities are very low at the front of a motor (see the correlation in Fig. 18), even

Table 4 Motor size effect on r_e using different scaling methods

Port diam., cm	r_e , cm/s		
	$D_h^{-0.2}$	$f(D_h)$	G_λ
1.27	0.498	0.498	0.498
2.54	0.450	0.465	0.249
12.7	0.335	0.330	0.051
25.4	0.312	0.178	0.025
50.8	0.279	0.071	0.013
127	0.239	0.013	0.005

**Fig. 19** Correlation of erosive behavior of different propellants.

though the Reynolds number far exceeds the transition value. The cause of the apparent threshold in the Saderholm data is not presently explainable. From an engineering viewpoint a threshold effect has a negligible influence on pressure prediction because it only affects a small fraction of the burning area.

Scaling

The L&R analysis is of interest because there have been a number of papers that correlated data based on using the L-R equation,⁶ and it has the only theoretical scaling parameter. Also, one of the few highly aluminized propellant erosive burning data is that of Lawrence et al.,³⁹ who correlated his results using that equation. Unfortunately, Lawrence only presents the final equation and not the original data, but he does give the nonerosive propellant properties. One of the propellants appears to be the Titan IIIC SRM propellant. At ignition the aft-end static pressure of that motor is about 5.17 MPa and $M \approx 0.3$. Lawrence gives the following information: $r_o = 1.02$ cm/s at 6.895 MPa, $n = 0.30$, $\alpha = 6.13$ cm^{2.8}k_g^{-0.8}s^{-0.2}, and $\beta = 70$, with initial bore diameter = 1.27 cm.

Lawrence modified the original L&R equation by replacing length with diameter. The equation is

$$r_e = \alpha G_c^{0.8} D_h^{-0.2} \exp(-\beta r_T \rho_s / G_c) \quad (17)$$

Assuming Lawrence used r_T in correlating the data, one can determine that at Titan IIIC SRM aft-end conditions Lawrence obtained $r_e = 0.498$ cm/s. One can now calculate the effect of motor size on r_e using three different methods, as shown in Table 4.

The first column uses Eq. (17) as written. The second column substitutes $f(D_h)$ as a suggested equation² to correct for motor size effect because the use of $D_h^{-0.2}$ overestimates erosive burning as motor size increases. The correct equation, which should be substituted for $D_h^{-0.2}$, is

$$f(D_h) = 0.5^{-0.2} \{0.90 + 0.189 D_h [1 + 0.043 D_h (1 + 0.023 D_h)]\}^{-1} \quad (18)$$

The third column calculates G_λ using Eq. (9) and assumes r_e varies linearly with G_λ because the average slope of all of the correlations (excluding the high value in Fig. 14) is 0.999. Although Eq. (9) underestimates u_λ , it appears to give satisfactory scaling although perhaps somewhat optimistic. Applying Van Driest's equation, Eq. (16), is difficult because scaling a Titan segment to a

1.27-cm bore diameter results in a grain length of about 4 cm, and the grain length was not given. The third column shows a faster decrease with port diameter than $f(D_h)$. The static pressure decrease in the SRM is about 12%, and so an erosion rate of 0.035 cm/s is necessary for the front and aft ends to have the same burning rate. It would be relatively simple to test these predictions using Bates motors and varying the initial port diameter because tests with port diameters from 1.27 to 25.4 cm would be sufficient. These results would also be useful in evaluating the flame zone thickness calculation.

Motor Design Application

Solid-propellant motor manufacturers have proprietary grain design and ballistic programs and can easily adapt the equations presented here to accommodate erosive burning. Equations such as those that produced Fig. 17 are easily developed, and algorithms to determine constants as a function of pressure and channel dimensions can be obtained simply. Even though Eq. (9) results in an incorrect velocity, the technique appears to give approximately the correct scaling for r_e as a function of port diameter.

SPP (Ref. 2) has another erosive burning equation (z and U_{th} are input values):

$$r_e = r_o [(U_c / U_{th})^z - 1] \quad (19)$$

This is easily rewritten:

$$r_T / r_o = (U_c / U_{th})^z \quad (20)$$

Using a correlation for formulation 4525,

$$r_T / r_o = 0.527 G_\lambda^{0.309} \quad (21)$$

Select the expected pressure to determine the gas density, and u_λ / U_c ,

$$r_T / r_o = 0.527 \rho_g^{0.309} (u_\lambda / U_c)^{0.309} U_c^{0.309} \quad (22)$$

At U_{th} , $r_T / r_o = 1$, and

$$1 / U_{th}^{0.309} = 0.527 \rho_g^{0.309} (u_\lambda / U_c)^{0.309} \quad (23)$$

Equation (23) can be solved for U_{th} for use in Eq. (19).

Using the same data that were used in the CFD analysis, $U_{th} = 2691$ in./s (68.35 m/s), $z = 0.499$ overpredicted the peak pressure of Fig. 1 by 7%. Increasing U_{th} to 3000 in./s (76.20 m/s) gave an almost perfect fit. This is useful to evaluate design options.

The laboratory correlations presented in this paper were used to calculate r_e at constant conditions ($P = 6.985$ MPa, $L = 20$ cm, $M = 0.3$) and plotted against the base burn rate (see Fig. 19). This plot supports the original suggestion that r_e should decrease as r_o increases. It also supports the generalization that at similar flow conditions r_e will be similar for many propellants. This correlation should be useful for estimating the erosive burning of new formulations.

Conclusions

A qualitative theory has been introduced, which explains the following: 1) that faster burning rate propellants appear less prone to erosive burning because the erosive burning is the same but the base burn rate has increased; 2) that the erosive burning rate decreases as the base burn rate increases because the turbulence will be less at the flame zone and it is more difficult to increase the heat flux of a faster burning propellant; 3) that propellants with similar burning rates have similar erosive behavior because the erosive burning rate is primarily dependent upon the flow conditions; and 4) that erosive burning is lower in larger motors because the gas velocities causing turbulence are lower at the flame zone. The last statement is supported by Van Driest's³⁸ prediction of the gas velocities in a laminar boundary developing on a flat plate with compressible flow. The gas velocities determined from Culick's¹⁹ analysis and used for scaling are shown to be too low, but the procedure is still applicable for scaling. It is shown that the published erosive burning data can be correlated in the form $r_e = K_1 G^{K_2}$. This provides useful equations

for the ballistician. Because the average value of $K2 \cong 1$, it is not surprising that linear plots of r_e , or r_T/r_o , vs G_c are found in the literature. The threshold effect is examined, and it is suggested that it occurs because the velocities in the boundary layer are still very low at the head-end of the motor even though the calculated Re_d far exceeds the usual transition value. A procedure for using the information presented is suggested for solid-propellant manufacturers and for those with less sophisticated programs like SPP (Ref. 2). To better understand erosive burning and to develop a viable scaling methodology, a better understanding of the velocity profile in the boundary layer in motors and in the laboratory experiments is necessary.

References

- ¹Saderholm, C. A., "A Characterization of Erosive Burning for Composite H-Series Propellants," AIAA Paper 64, Jan. 1964.
- ²Dunn, S. S., Coats, D. E., and French, J. C., "SPP 97TM 3D Grain Design User's Manual," Software and Engineering Associates, Inc., Carson City, NV, Jan. 2001.
- ³Wang, J., Landsbaum, E., Cozart, A., Frolik, S., and Lee, I., "Recent Progress in SRM Ignition Transient Modeling," AIAA Paper 2003-5115, July 2003.
- ⁴Razdan, M. K., and Kuo, K. K., "Erosive Burning in Solid Propellants," *Fundamentals of Solid Propellant Combustion*, edited by K. K. Kuo and M. Summerfield, Progress in Astronautics and Aeronautics, Vol. 90, AIAA, New York, 1984, pp. 515–598.
- ⁵Green, L., "Erosive Burning of Some Composite Solid Propellants," *Jet Propulsion*, Vol. 24, No. 1, 1954, pp. 9–15.
- ⁶Lenoir, J. M., and Robillard, G., "A Mathematical Method to Predict the Effects of Erosive Burning in Solid Propellant Rockets," *Proceedings of the Sixth (International) Symposium on Combustion*, Reinhold, New York, 1957, pp. 663–667.
- ⁷Razdan, M. K., and Kuo, K. K., "Erosive Burning Study of Composite Solid Propellants by Turbulent Boundary Layer Approach," *AIAA Journal*, Vol. 17, No. 11, 1979, pp. 1225–1223.
- ⁸Jacobs, P. W. M., and Whitehead, H. M., "Decomposition and Combustion of Ammonium Perchlorate," *Chemical Reviews*, Vol. 69, 1969, pp. 551–590.
- ⁹Varney, A. M., and Strahle, W. C., "Thermal Decomposition Studies of Some Solid Propellant Binders," *Combustion and Flame*, Vol. 16, No. 1, 1971, pp. 1–8.
- ¹⁰Lengelle, G., "Thermal Degradation Kinetics and Surface Pyrolysis of Vinyl Polymers," *AIAA Journal*, Vol. 8, No. 11, 1970, p. 1995.
- ¹¹Bevilacqua, E. M., "Thermal and Oxidative Degradation of Natural Rubber and Allied Substances," *Thermal Stability of Polymers*, edited by R. T. Conley, Monographs in Macromolecular Chemistry, Vol. 1, Marcel Dekker, New York, 1970, p. 192.
- ¹²Yamada, K., Goto, M., and Ishikawa, N., "Simulative Study on the Erosive Burning of Solid Rocket Motors," *AIAA Journal*, Vol. 14, No. 9, 1976, pp. 1170–1177.
- ¹³King, M. K., "Predicted and Measured Effects of Pressure and Crossflow Velocity on Composite Propellant Burning Rate," *Proceedings of the 17th Combustion Meeting*, CPIA Pub. 329, Vol. I, 1980, pp. 99–122.
- ¹⁴Beddini, R. A., "Effect of Grain Port Flow on Solid Propellant Erosive Burning," AIAA Paper 78-977, July 1978.
- ¹⁵Friedman, R., "Experimental Techniques for Solid-Propellant Combustion Research," *AIAA Journal*, Vol. 5, No. 7, 1967, p. 1217.
- ¹⁶Software and Engineering Associates, Carson City, NV.
- ¹⁷Kishore, K., and Gayathri, V., "Chemistry of Ignition and Combustion of Ammonium-Perchlorate-Based Propellants," *Fundamentals of Solid-Propellant Combustion*, edited by K. K. Kuo and M. Summerfield, Progress in Astronautics and Aeronautics, Vol. 90, AIAA, New York, 1984, p. 91.
- ¹⁸White, F. M., *Fluid Mechanics*, McGraw-Hill, New York, 1979, Chaps. 6 and 7.
- ¹⁹Culick, F. E. C., "Rotational Axisymmetric Mean Flow and Damping of Acoustic Waves in a Solid Propellant Rocket," *AIAA Journal*, Vol. 4, No. 8, 1966, pp. 1462–1464.
- ²⁰Dunlap, R., Willoughby, P. G., and Hermesen, R. W., "Flowfield in the Combustion Chamber of a Solid Propellant Rocket Motor," *AIAA Journal*, Vol. 12, No. 10, 1974, pp. 1440–1442.
- ²¹King, M. K., "Erosive Burning of Solid Propellants," *Journal of Propulsion and Power*, Vol. 9, No. 6, 1993, pp. 785–805.
- ²²Marklund, T., and Lake, A., "Experimental Investigation of Propellant Erosion," *ARS Journal*, Vol. 3, No. 2, 1960, pp. 173–178.
- ²³Strand, L., Yang, C., Ray, R., and Barry, J., "Erosive Burning Research," *22nd JANNAF Combustion Meeting*, CPIA Pub. 432, Vol. 1, Oct. 1985, pp. 29–40.
- ²⁴Strand, L., and Cohen, N., "Erosive Burning Threshold Conditions in Solid Rocket Motors," AIAA Paper 89-2528, July 1989.
- ²⁵McComb, J. C., Behm, J. W., Hocutt, S. R., McKay, R. A., Rivkin, S. R., Strand, L. D., Compton, L. E., and Anderson, F. A., "ASRM Propellant Composition Tradeoff Study," Jet Propulsion Lab., JPL D-8765, Pasadena, CA, Aug. 1991.
- ²⁶Martin, C. L., "Evidence of Erosive Burning in Shuttle Solid Rocket Motor," *1983 JANNAF Propulsion Meeting*, CPIA Pub. 370, Vol. 1, pp. 7–13.
- ²⁷Price, E. W., and Sigman, R. K., "Combustion of Aluminized Solid Propellants," *Solid Propellant Chemistry, Combustion, and Motor Interior Ballistics*, edited by V. Yang, T. B. Brill, and Wu-Zhen Ren, Progress in Astronautics and Aeronautics, Vol. 185, AIAA, New York, 2000, pp. 663–688.
- ²⁸Razdan, M. K., and Kuo, K. K., "Measurements and Model Validation for Composite Propellants Under Crossflow of Gases," *AIAA Journal*, Vol. 18, No. 6, 1980, pp. 669–677.
- ²⁹Robillard, G., and Lenoir, J. M., "The Development of a New Erosive Burning Law," Jet Propulsion Lab., Publication No. 91, Pasadena, CA, 1 April 1957.
- ³⁰Godon, J. C., Duterque, J., and Lengelle, G., "Solid Propellant Erosive Burning," *Journal of Propulsion and Power*, Vol. 8, No. 4, 1992, p. 741.
- ³¹Godon, J. C., Duterque, J., and Lengelle, G., "Erosive Burning in Solid Propellant Motors," *Journal of Propulsion and Power*, Vol. 9, No. 6, 1993, pp. 806–811.
- ³²Ruiz, H., Sautereau, K., and Tissier, P. Y., "Experimental Investigation and Numerical Modeling of Erosive Burning in Solid Rocket Motors," AIAA Paper 96-2642, July 1996.
- ³³Kamath, H., Arora, R., and Kuo, K. K., "Erosive Burning Measurements and Predictions for a Highly Aluminized Composite Solid Propellant," AIAA Paper 82-1111, June 1982.
- ³⁴Cebici, T., and Smith, A. M. O., *Analysis of Turbulent Boundary Layers*, Academic Press, New York, 1974, p. 136.
- ³⁵Beddini, R. A., "On the Scaling of Solid Propellant Erosive Burning: The Threshold Condition," *Proceeding of the 15th JANNAF Combustion Meeting*, CPIA Pub. 297, Vol. II, 1979, pp. 199–216.
- ³⁶Schlichting, H., *Boundary-Layer Theory*, McGraw-Hill, New York, p. 607.
- ³⁷White, F. M., *Viscous Fluid Flow*, McGraw-Hill, New York, 1974, pp. 592, 263.
- ³⁸Van Driest, E. B., "Investigation of Laminar Boundary Layers in Compressible Flow Using the Crocco Method," North American Aviation, Inc., NACA Technical Note 2597, Jan. 1952.
- ³⁹Lawrence, W. J., Matthews, D. R., and Deverall, L. I., "The Experimental and Theoretical Comparison of the Erosive Burning Characteristics of Composite Propellants," AIAA Paper 68-531, June 1968.